Longitudinal characterization of blood-brain barrier permeability after experimental traumatic brain injury by *in vivo* 2-photon microscopy

Yue Hu,[1,3,4] Burcu Seker,[1,4] Carina Exner,[1,4] Junping Zhang,[3] Nikolaus Plesnila,[1,4*] and Susanne M. Schwarzmaier,[1,2,4]

[1]Institute for Stroke and Dementia Research (ISD), Ludwig-Maximilians-University (LMU) Munich Medical Center, Munich, Germany

[2]Department of Anesthesiology, Ludwig-Maximilians-University (LMU) Munich Medical Center, Munich, Germany

[3]First Teaching Hospital of the Tianjin University of Traditional Chinese Medicine, Tianjin, China,

[4]Cluster for Systems Neurology (SyNergy), Munich, Germany

***corresponding author**

Running title: BBB permeability after experimental TBI

Table of contents title: BBB permeability after TBI assessed by in vivo microscopy

Addresses:

Yue Hu, Institute for Stroke and Dementia Research, Feodor-Lynen-Str. 17, 81377 Munich, Germany, huyue@yahoo.com

Burcu Seker, PhD, Institute for Stroke and Dementia Research, Munich University Hospital, Feodor-Lynen-Str. 17, 81377 Munich, Germany,

burcu.seker@med.unimuenchen.de

Carina Exner, Institute for Stroke and Dementia Research, Feodor-Lynen-Str. 17, 81377 Munich, Germany, Carina.Exner@med.uni-muenchen.de

Junping Zhang, PhD, Department of Geriatrics, First Teaching Hospital of Tianjin University of Traditional Chinese Medicine, 314 An Shan Xi Road, Nan Kai District, Tianjin 300193, China,

tjzhtcm@163.com

*Nikolaus Plesnila, MD, PhD, Institute for Stroke and Dementia Research, Feodor-Lynen-Str. 17, 81377 Munich, Germany, Tel: +49 89 4400 46220, Fax: +49 89 4400 46113, nikolaus.plesnila@med.uni-muenchen.de

Susanne M. Schwarzmaier, MD, Institute for Stroke and Dementia Research & Department of Anesthesiology, University of Munich Medical Center, Marchioninistr. 15, 81377 Munich, Germany,

Susanne.Schwarzmaier@med.uni-muenchen.de

Abstract

Vasogenic brain edema formation remains an important factor determining the fate of patients suffering from traumatic brain injury (TBI). The spatial and temporal development of VBE, however, remain poorly understood due to the lack of sufficiently sensitive measurement techniques. To close this knowledge gap, we directly visualized the full time course of vascular leakage following TBI by *in vivo* 2-photon microscopy (2-PM).

Male C57BL/6 mice (n=6/group, 6-8 weeks old) were randomly assigned to sham-operation or brain trauma by Controlled Cortical Impact. A cranial window was prepared and tetramethylrhodamine-dextran (TMRM, MW 40,000 Da) was injected intravenously to visualize blood plasma 4, 24, 48, 72h, or 7d after surgery or trauma. Three regions with increasing distance to the primary contusion were investigated up to a depth of 300 µm by 2-PM.

No TMRM extravasation was detected in sham-operated mice, while already 4h after TBI vascular leakage was significantly increased ($p<0.05$ vs. sham) and reached its maximum at 48h after injury. Vascular leakage was most pronounced in the vicinity of the contusion. The rate of extravasation showed a biphasic pattern, peaking 4h and 48-72h after trauma.

Taken together, longitudinal quantification of vascular leakage after TBI *in vivo* demonstrates that vasogenic brain edema formation after TBI develops in a biphasic manner suggestive of acute and delayed mechanisms. Further studies using the currently developed dynamic *in vivo* imaging modalities are needed to investigate these mechanisms and potential therapeutic strategies in more detail.

Key words: traumatic brain injury; vasogenic brain edema; blood brain barrier; *in vivo*; 2-photon microscopy

Introduction

Traumatic brain injury (TBI) remains a growing public health concern worldwide and across all ages with a disproportionate burden of disability and mortality occurring in children and young adults. [1, 2] Despite the medical, surgical, and rehabilitation interventions that have been developed and improved for treating TBI, numerous patients with severe head trauma still suffer from unfavorable outcomes including death or long-term disability. [3-5]

A key factor in the pathogenesis of secondary brain damage is brain edema formation contributing to brain swelling. After exceeding the intracranial compliance, brain swelling leads to an increase in intracranial pressure (ICP), which in turn results in global cerebral ischemia and further tissue damage. [5-11]

Classically, TBI-induced brain edema has been categorized as 'vasogenic' or 'cytotoxic'. [12-14] Cytotoxic edema is characterized by an intracellular water accumulation of astrocytes, neurons, and microglia. [8, 10, 14] In short, cells take up solutes in order to maintain extracellular ion homeostasis and this process results in an osmotic-driven water influx. Water moves from the interstitial to the intracellular space, thereby causing cell swelling. [13, 15] Vasogenic brain edema (VBE) occurs when the permeability of the blood-brain barrier (BBB) is increased. [11] Driven by hydrostatic pressure, water together with plasma proteins and electrolytes leaks into the interstitial compartments with ensuing water accumulation. [8, 14, 16] This results in brain swelling and eventually life-threatening intracranial hypertension. [9, 17-19]

To date, the spatial and temporal development of vasogenic brain edema formation following brain trauma has been controversial. [8, 10, 14, 20] The main reasons for this situation were technical limitations which did not allow to measure VBE formation with a sufficiently high temporal and spatial resolution. For example, VBE was investigated *ex vivo* by Evan's blue

extravasation, which allowed no dynamic characterization, or *in vivo* by epifluorescence microscopy, which was limited to an investigation of pial vessels located on the brain surface. [8, 10] These limitations were overcome by *in vivo* 2-photon microscopy (2-PM), a technology which allows a detailed temporal characterization of VBE formation with subcellular resolution in 3D. [21] Hence, the aim of the current study was to use 2-photon *in vivo* imaging to characterize the full time course of the formation of VBE following TBI, i.e. from immediately after TBI until a week thereafter.

Materials and Methods

Animal and Husbandry

All protocols and procedures on animals were approved by the Government of Upper Bavaria and are reported in accordance with the ARRIVE (Animal Research: Reporting of in vivo Experiments) guidelines. Male 6-8-week-old C57Bl/6 mice with a body weight of 22-26 g (Charles River Laboratories, Germany) were used for the current experiments. Animals were housed in groups of up to five per cage under a 12-hour light/dark cycle with free access to food and water. Health screens and hygiene management checks were performed daily in accordance with the guidelines and recommendations established by the Federation of European Laboratory Animal Science Associations (FELASA).

Experimental protocol

Seven experimental groups with six mice each were investigated. Five groups were subjected to TBI and allowed to wake up from anesthesia immediately thereafter. Two, 22, 46, 70 or 166 hours later animals were re-anesthetized, a cranial window was prepared, and blood brain barrier permeability was investigated by *in vivo* 2-photon microscopy four, 24, 48, 72 hours and seven days after TBI (**Fig. 1A**). At the end of the experiment blood gases were assessed.

Subsequently, mice were sacrificed in deep anesthesia by cervical dislocation, brains were removed and photographed, and brain water content was determined by the wet-dry method. In two experimental groups mice were subjected to sham surgery and allowed to survive for 2 hours or seven days. In the two groups observed for seven days (sham and TBI) body weight and functional outcome was assessed on days one, two, three, and seven.

Randomization and Blinding

For each series of experiments, mice were randomly assigned to the treatment group after preparation of the craniotomy by drawing lots. The 2-PM imaging and analysis was performed by a researcher blinded with respect to the treatment.

Experimental TBI Model

TBI was induced as described previously by using the Controlled Cortical Impact (CCI) procedure. [21-23] Briefly, animals received a subcutaneous injection of Buprenorphine (0.1 mg/kg) for analgesia, were anesthetized with Isoflurane (1,5-1,8% in room air with 30% O_2), and fixed in a stereotactic frame using a palate plate holder (Model 921-E, David Kopf Instruments, Tujunga, USA). A feedback controlled heating pad (40908D01, FHC, Bowdoin, USA) was used to maintain body temperature at 37°C. Following a longitudinal skin incision along the sagittal suture, a craniotomy of 4 x 4mm was prepared posterior-lateral to bregma over the right parietal cortex (**Fig. 1B**). The impact was applied perpendicular to the dura with a cylindrical impactor (diameter: 3.0 mm), a velocity of 6 m/sec, a penetration depth of 0.5 mm, and a contact time of 150 ms with a custom made digitally controlled electro-pneumatic CCI device (L. Kopacz, University of Mainz, Germany). Immediately following the impact, the removed bone flap was repositioned and fixed with tissue glue. The skin was sutured and the mice were placed in a recovery chamber heated to 32°C (CA17 4BG, Mediheat^{TM}, UK) to

prevent postoperative hypothermia until full recovery of motor function. Sham-operated animals were treated as described above except for the induction of CCI.

Cranial Window Preparation

Mice were anesthetized by intraperitoneal injection of 0.05 mg/kg Fentanyl, 0.5 mg/kg Medetomidine, and 5 mg/kg Midazolam and intubated with a custom-made tube connected to a volume-controlled ventilator (Minivent 845, Hugo Sachs Electronic, Germany) and a microcapnometer (PhysioSuite, Kent Scientific, Torrington, USA) as described previously. [21] Ventilation volume and respiratory frequency were adjusted according to body weight and end tidal pCO_2. Body temperature was maintained with a feed-back controlled heating pad (40908D01, FHC, Bowdoin, USA). The head was fixated in a nose clamp mounted on a stereotactic frame (Model 902, David Kopf Instruments, Tujunga, USA). For measurement of the blood pressure a sterile plastic catheter was inserted into the femoral artery and connected to a pressure transducer. Animals received 0.4 ml/h 0.9% NaCl via a femoral catheter to account for ventilation-induced fluid loss. Body temperature, mean arterial blood pressure (MABP) and end-tidal pCO_2 were recorded digitally throughout the experiment and stored for further analysis (Powerlab, ADInstruments, Sydney, Australia).

A square cranial window (2mm x 2mm) was prepared as previously described. [21] Briefly, a craniotomy was drilled carefully over the right fronto-parietal cortex 1 mm lateral to the sagittal suture and 1 mm frontal to the coronal suture (**Fig. 1B**) under continuous cooling with saline. Special care was taken to leave the dura mater intact. After removal of the bone flap, the dura mater was gently removed and the surface of the brain was rinsed with saline. Then, a fitting square cover glass (LOT 2441285, Thermo Fisher Scientific, USA) with a thickness of 175 µm was carefully placed within the craniotomy and fixed with dental cement. The caudal

rim of cranial window was 1.5 mm rostral to the primary contusion, i.e. over the traumatic penumbra.

Two-photon Microscopy

In vivo imaging was performed as previously described. [21] Briefly, after preparation of the cranial window anesthesia and monitoring were continued and mice were placed under a 2-photon microscope (Zeiss LSM 7MP). For imaging, mice received an i.a. injection of 40 mg/kg tetramethylrhodamine-dextran (TMRM; MW 40,000, Invitrogen, Darmstadt, Germany). The molecular weight of 40,000 Dalton was specifically chosen because molecules of that size can cross the blood brain barrier exclusively under pathological conditions. [24, 25] TMRM was exited at 800 nm and fluorescence was recorded at 500–550 nm. In order to provide an even signal intensity throughout the 3D region of interest, the laser power was depth-dependent adjusted from 3-15%. Master and digital gain were set 650 and 2.00, respectively. These settings were determined empirically in order to visualize the vessels and parenchyma in a 3D region of interest reaching 0–300 micrometers below the surface with equal intensity and minimal background fluorescence.

For imaging, three regions of interest (ROI) were defined within the cranial window (**Fig. 1C**). Area 1 (A1) was the ROI closest to the site of primary damage (1.5 mm frontal to the rim of the initial contusion). Area 2 (A2) and area 3 (A3) were located at a distance of 2 mm and 2.5 mm from the rim of the contusion, respectively. The horizontal/x-y dimension of each of the three ROIs was 425 µm x 425 µm and 100 images were recorded every 3 µm up to depth of 300 µm. Three-dimensional image stacks (z-stacks) were reconstructed off-line. Baseline images were captured from each ROI within two minutes after injection of TMRM. Thereafter,

z-stacks of each ROI were obtained every 30 minutes. At the end of each experiment, arterial blood gases and pH were measured (Rapidlab 348; Siemens, Munich, Germany).

Neurological monitoring

Body weight, the state of consciousness, behavior, wound condition, and the general clinical condition were evaluated daily for the first 3 days and on the 7th day after trauma using a neurological score (see table 2).

Brain Water Content Measurement

Brain water content was determined by the wet-dry method as previously described. [26] Briefly, animals were sacrificed in deep anesthesia by cervical dislocation. Brains were quickly removed, placed on a metal matrix cooled to 4°C, the olfactory bulb and the cerebellum were removed, and hemispheres separated. Wet (W) and dry (D) weight was determined before and after drying the tissue at 110°C for 24 hours, respectively. Brain water content was calculated in % using the following formula: (W-D)/Wx100

Quantification of 2-PM Images

Image analysis was performed off-line using the software ImageJ by an investigator blinded to the treatment of the animals. [21] To avoid a bias from potential surgical trauma to the brain surface by preparation of the cranial window, the superficial 50 µm of each z-stack were excluded from the analysis. The intensity threshold was adjusted to eliminate both the very high intravascular signal and the very low background signal present in all images. Adjustments were standardized and uniformly applied to all datasets. Subsequently, fluorescent pixels were counted in each z-stack using ImageJ. Fluorescence of each z-stack was then determined as the mean value of each section. Baseline fluorescence intensity was determined in the z-stack that was acquired immediately after TMRM injection. To measure

the extravasation distribution, the original data (z-stack) was transferred into the maximal intensity projection form by applying a specific look-up-table (jet color map) into the image. Then, each image was gridded into 36 segments (6 X 6). In each segment, a ROI in the parenchyma was chosen (excluding vessels). The fluorescence intensity was measured within each ROI using ImageJ. All following measurements were expressed as % baseline.

In order to determine extravasation rate, i.e. the amount of TMRM extravasation per minute, the following formula was used: *(Fluorescence intensity at 90 min – baseline fluorescence intensity)/90 min.* The results are presented *as change of fluorescence intensity per minute.*

Statistical Analysis

Group sizes were calculated with a standard deviation of 25% of the mean, a biologically relevant detection limit of 50%, and a power of 0.8. Statistical analysis was performed using GraphPad Prism 6.0. To follow the most conservative approach possible, non-parametrical tests were used throughout even when single data sets passed normality and equal variance testing. Hence, the Mann-Whitney U test was used to analyze the differences between groups and the Kruskal–Wallis analysis of variance on ranks was used to compare more than two groups. All data are presented as means ± standard deviation (SD). Differences with *P* values less than 0.05 were considered to be statistically significant.

Results

Brain swelling after TBI

As a clinical parameter reflecting brain edema we assessed the midline shift (**Fig. 2A**). Swelling of the traumatized hemisphere was already visible four hours after TBI. At 48 hours after injury the midline shift reached its maximum and decreased thereafter. Seven days after TBI no midline shift was detectible any more. Additionally, hematoma was visible on the brain

surface. The same brains were used to determine brain water content by using the wet-dry method (**Fig. 2B**). Sham operated mice (n=6) had a normal brain water content of 78.3±0.5%. Four hours after TBI brain water content of the traumatized hemisphere increased by 2.1% to 80.4±0.8% (n=6; $p<0.05$ vs. sham). Thereafter, the water content of the traumatized hemisphere further increased to about 81% 24 hours after trauma and remained on this level for at least 48 hours (n=6; $p<0.05$ vs. sham). 72 hours after TBI brain water content slightly decreased and reached values not significantly different from baseline values seven days after injury (79.5±1.1%, n=6; n.s. vs. sham and contralateral hemisphere).

Characterization of acute vasogenic brain edema formation 4 h after TBI

Physiological monitoring

Surgery and 2-photon imaging lasted up to 4 hours. To ensure that all measurements were performed under physiological conditions, body temperature, mean arterial blood pressure and end-tidal CO_2 were continuously monitored and controlled. All values were within their respective physiological range and showed no significant difference between experimental groups (**Suppl. figures 1A-1C**). At the end of the experiment, blood gases including pH, pCO_2 and pO_2 were measured. pCO_2 and pO_2 were within their physiological range and did not differ between groups (**Tab. 2**). Animals in both experimental groups developed a slight acidosis with a pH of 7.2.

Temporal and spatial profile of TMRM extravasation 4h after TBI

A control image serving as baseline for all subsequent measurements was acquired immediately after TMRM injection. No extravasation was detected in sham-operated mice (**Fig. 3A, upper panels**). Four hours after TBI TMRM fluorescence started to increase in the brain parenchyma 30 minutes after injection of the tracer as a signs of vascular leakage (**Fig.**

3A, lower panels). Quantification of dye leakage in the three predefined regions of interest A1-A3 demonstrated that fluorescence intensity increased only in the two ROIs adjacent to the contusion (A1 and A2; **Fig. 3B and C;** $p<0.05 – 0.01$), while in the ROI most distant to the contusion vascular leakage was quite limited at this time point. Hence, vessel permeability or edema fluid spread in a centripetal manner from the rim of the contusion.

In addition to the horizontal distribution of vascular leakage, 2-photon microscopy allowed us to assess vascular leakage up to 300 µm below the surface of the brain. No extravasation of TMRM was observed after sham operation (**Fig. 4A**), however, after TBI TMRM extravasation was not only observed in the superficial layers of the cortex (<100 µm below the surface), but down to a depth of 250 µm (**Fig. 4B**). Again, four hours after TBI vascular leakage was only observed in the two ROIs closest to the rostral rim of the contusion. Therefore, these data suggest, that after TBI vascular leakage occurs in a progressive manner temporally as well as spatially.

Characterization of sub-acute brain edema formation 24h to 7 days after TBI

General conditions after TBI

As a parameter of general wellbeing, we measured body weight before and after surgery. No significant changes were observed within or between groups (**Suppl. Fig. 2A**). We also quantified the general condition of the mice using a behavioral score assessing general behavior, general condition, weight loss, neurologic deficits, wound conditions, vigilance, and epileptic seizures on days 1, 2, 3, and 7 (**Table 1**). On the first day following TBI traumatized mice had a higher behavioral score as compared to sham orated animals ($p<0.05$ vs. sham; **Suppl. Fig. 2B**). Afterwards, mice recovered quickly and no abnormal behavior was observed after day three in either group.

Physiological parameters during and after imaging

As in the experiments investigating the development of VBE 4-6 hours after TBI, body temperature, mean arterial blood pressure, and end-tidal CO_2 were also monitored in the sub-acute cohorts. All values were within their respective physiological range and showed no significant difference between groups (**Suppl. Figs. 3A-C**). Also blood gas values were within their respective physiological range and did not differ significantly between groups. However, in this experimental series blood pH was slightly acidotic (**Table 3**).

Temporal profile of TMRM extravasation

As observed in the acute cohort, sham operated animals did not show any TMRM extravasation throughout the experiment (**Fig. 5A, upper panels**). 24, 48, and 72 hours after trauma, parenchymal fluorescence intensity increased within ROI A1. Seven days after TBI almost no parenchymal fluorescence could be detected (**Fig. 5A, lower panels**). Quantification of parenchymal fluorescence intensities in ROIs A1, A2, and A3 confirmed these observations (**Fig. 5B and 6**). No extravasation of TMRM was observed in sham operated mice and seven days after TBI, while 24, 48, and 72 hours after head injury dye leakage was observed in all three ROIs. When comparing peak extravasation values over time, TMRM extravasation was most prominent at 48 hours following CCI (P<0.01, vs sham, **Fig. 6F**). Only at this time point extravasation was also significantly elevated in A3, the ROI most distant to the rostral rim of the contusion (P<0.05 vs baseline).

Spatial distribution of VBE formation following trauma

To determine whether vascular leakage was also present in deeper cortical layers, TMRM extravasation was determined in five 50 µm thick ROIs located from the surface of the cortex down to a depth of 300 µm. No extravasation was observed in sham-operated animals and

seven days following trauma (**Fig. 7A and E**). One day after injury, TMRM extravasation was most dominant in superficial cortical layers (<200 µm; P<0.05-0.01 vs sham; **Fig. 7B**). Two and three days after TBI vascular leakage extended to deeper cortical layers (200-300 µm), mainly in the two ROIs next to the contusion (P<0.05-0.01 vs sham; **Fig. 7C and D**).

Characterization of extravasation rate after TBI

So far, we determined the amount of TMRM extravasated into the brain parenchyma. Since, however, we measured the extravasation of TMRM dynamically for 90 min at each investigated time point, we were also able to determine the extravasation rate of TMRM, i.e. a measure for the actual permeability of the blood brain barrier. Due to the spatial resolution of our microscopic approach, the extravasation rate could be determined for each ROI (**Fig. 8**). No extravasation was observed after sham operation and seven days after TBI. Interestingly, the extravasation rate peaked 4 and 48 hours after head injury; only in ROIs A1 and A2, i.e. next to the contusion, at four hours after injury and in all three ROIs 48 hours after trauma. This pattern suggests that the blood-brain barrier opens in a bi-phasic manner following TBI; once early after injury and a second time two days after trauma.

Discussion

In the present study, we used *in vivo* 2-photon microscopy to investigate the amount and the rate of extravasation of a fluorescent dye injected into the blood stream of mice at different time points after experimental traumatic brain injury. Using this technique, we were able to determine the amount of the plasma protein marker extravasation into the brain parenchyma and to quantify the permeability of the blood-brain barrier after TBI *in vivo*. Our data demonstrate opening of the blood brain barrier (BBB) to large plasma proteins (40 kDa) as early as four hours after TBI. BBB opening lasted at least for three days and was accompanied

by a significant increase in brain water content. BBB permeability followed a biphasic pattern, with an early peak four and a more delayed peak from 48-72 hours following injury, suggesting that vasogenic brain edema formation may be mediated by different mechanisms over time. More importantly, the current study demonstrates that vasogenic brain edema formation can be directly visualized and quantified in a dynamic manner *in vivo,* thereby paving the way for future therapeutic and mechanistic studies after TBI and other neurological disorders.

Cerebral edema is defined as an increase of brain tissue water content. [10] Vasogenic brain edema occurs due to the extravasation of plasma proteins and water from the vascular compartment into the brain parenchyma. When brain swelling exceeds the intracranial compliance, intracranial hypertension occurs and causes perfusion deficits. This is associated with unfavorable outcome following TBI. [6-8, 10, 14, 20, 27, 28] Consequently, brain edema formation has been in the focus of neuroscience research for decades. However, our knowledge about time course, significance, and mechanisms of vasogenic brain edema formation remains quite limited, e.g. until recently not even the precise vascular source of vasogenic edema was known.[21] The main reason for our only partial understanding of vasogenic edema are technical limitations, i.e. lack of technologies which allow to investigate BBB permeability with a high spatial and temporal resolution longitudinally *in vivo*. Previously used techniques to investigate TBI-induced BBB opening included determination of Evans blue or IgG extravasation *ex vivo*, [29, 30] and *in vivo* experiments using MRI, [31-33] epifluorescence microscopy [34-36] or near-infrared (NIR) fluorescence imaging. [37] However, the quantification of Evans blue extravasation requires the sacrifice of the animal under investigation and provides therefore only information about one single time point. Further, Evans Blue has a quite variable binding affinity to albumin and is therefore not an ideal marker for the investigation of BBB permeability. [38] Diffusion weighted imaging (DWI) provides good temporal and morphological

resolution *in vivo*, however, the temporal and spatial resolution of this technology are not good enough to determine the exact location and dynamics of BBB opening. Therefore, microscopic techniques using fluorescent tracers and allowing direct visualization of cerebral vessels in anesthetized animals were regarded as superior techniques for the investigation of the BBB. [34, 35] Depending on the tracers used, not only vessel permeability but also inflammatory cells could be observed with this technique. [36, 39-41] Conventional fluorescence microscopy, however, has such a low tissue penetration that only pial vessels can be investigated with this technique, i.e. those cerebral vessels which are not covered by astrocytes and may therefore not be ideal to study BBB permeability. [42] These limitations can be overcome by fluorescence microscopy techniques, which have higher tissue penetration, i.e. 2-photon microscopy (2-PM). 2-PM uses excitation wavelengths twice as long as conventional fluorescence microscopy and is therefore able to penetrate much deeper into biological tissues, i.e. up to 600 µm, without causing tissue damage. [43] Since 2-PM has also a decent resolution along the vertical axis (z-axis), intraparenchymal cerebral vessels, i.e. those vessels which actually form the BBB, can be visualized *in vivo* with high spatial and temporal resolution. We previously used 2-PM to investigate the vascular source of vasogenic brain edema formation after TBI and demonstrated that extravasation occurs in venules, arterioles, and capillaries. [21] Hence, we already demonstrated that the currently used setup is suitable to measure BBB permeability in parenchymal microvessels *in vivo*.

In the first part of the current study, brain swelling and edema formation were investigated *ex vivo* at different time points after experimental TBI. There was no edema formation in sham-operated animals, however, a rapid increase of water content was detected within the first four hours after CCI. Brain water content remained high in the ipsilateral hemisphere for at least three days and returned to normal values seven days after trauma. These results are

well in line with previously published data by us and others, and demonstrate that the trauma model used in the current study is well reproducible and yields results comparable to other laboratories. [26, 27]

As already discussed, the main advantage of the microscopic assessment of BBB permeability *in vivo* is the high spatial and temporal resolution of the technique while animals are kept under tightly controlled physiological conditions. This approach therefore allows the unambiguous visual assessment of microvascular permeability at various time points after TBI. Using other techniques, which rather employ surrogate markers for brain water content and vascular permeability, e.g. MRI, vasogenic brain edema formation was demonstrated to occur immediately after TBI and to last only up to 1 hour thereafter. [44] Consequently, vasogenic brain edema was discussed to be of minor relevance after TBI. [8] Using a technology which directly visualizes BBB permeability on the level of the cerebral microcirculation, we were now able to demonstrate that vasogenic brain edema formation indeed occurs in the traumatized brain for up to one week after trauma. Further studies using the current technology will need to address also later time points after TBI, since others reported a disruption of the BBB for weeks following experimental trauma [45-52] and some clinical studies even suggested the BBB permeability may be impaired for years after TBI. [53]

In addition to the question whether vasogenic edema plays a relevant role after TBI, also the time course of BBB opening was a matter of discussion. Using conventional techniques to assess vasogenic brain edema, e.g. extravasation of endogenous IgG, some groups reported wide spread opening of the BBB in the traumatized hemisphere within the first 24 hours after TBI, [21, 50] while others reported additional opening of the BBB 3-7 days following injury. [27, 54] The exact time course of BBB disruption after TBI may be related to the different TBI models

and animal species used to assess vasogenic edema formation, however, the used techniques may also have played a major role, i.e. dynamic *in vivo* measurements were not available so far. Using 2-PM, the current study demonstrates that brain edema formation indicated by TMRM extravasation increases following a cortical contusion within a few hours and remains elevated for at least three days after TBI. However, BBB permeability (as determined by the rate of dye extravasation) shows a bi-phasic pattern, i.e. the BBB opens within the first few hours after TBI, shows a partial closure 24 hours thereafter, and re-opens 2-3 days after injury. This bi-phasic pattern strongly suggests that vasogenic edema following TBI is very likely mediated by multiple mechanisms. The first peak may be mediated by the initial mechanical impact to the brain and the subsequent stretching of cerebral microvessels, which, depending on the applied force, may result in microvascular hemorrhage or just leakage of plasma proteins and water. [55] This process may be worsened by acute activation of neutrophils. [56-61] The second peak could be the result of a delayed, more chronic inflammatory processes involving macrophages and microglia initiated to remove damaged tissue and to repair the injured brain. [39] [59], [62] [63], [64]

In addition to the determination of the exact time course of vasogenic brain edema formation and BBB permeability changes, 2-PM offers also the possibility to determine the precise spatial distribution of vascular leakage after TBI. In the current study, we placed a cranial window 1.0–3.0 mm rostral to rim of a contusion. This allowed us to investigate vascular permeability in the traumatic penumbra down to a depth of 300 µm. Early after TBI, tracer extravasation occurred mainly within the vicinity of the contusion, suggesting that edema fluid may have extravasated locally or may have diffused from the site of the contusion into the imaging window. Based on our previous studies, where we clearly demonstrated vascular leakage four hours after TBI using high resolution vascular imaging, we could, however, exclude diffusion

of edema fluid as the source of tracer fluorescence. [21] Hence, local opening of the BBB within the traumatic penumbra is the most likely mechanism responsible for the detection of the vascular tracer under these circumstances. The same seems also to be the case at later time points after TBI. The homogenous and simultaneous appearance of the tracer in the whole ROI suggests local opening of the BBB rather than diffusion of edema fluid from the contusion into the penumbra. Since the ROI most distant to the contusion is affected by vascular leakage only 48 hours after TBI, an active mechanism opening and closing the BBB seems to occur. Which mechanisms are involved remains to be investigated in the future using the currently developed technique. Similar temporal and spatial changes occured not only superficially, but also within the cerebral cortex. Edema fluid extravasated within the vicinity of the contusion early after trauma and increases in more distant areas 2-3 days thereafter. Hence, spatial opening of the BBB after TBI seems to occur in a centripetal manner from the site of injury.

Taking together, vasogenic brain edema formation after TBI has an acute component most likely caused by mechanical stretch of cerebral microvessels. This early BBB disruption occurs in the vicinity of the injury site and results in an increase in brain water content. Following this early phase, the BBB seems to partially close and then reopen 2-3 days after trauma due to so far unknown secondary mechanisms. This second phase of BBB disruption is more widely spread and involves more distant brain areas than acute BBB disruption. Hence, we speculate that delayed inflammatory mechanisms drive secondary BBB disruption and subsequent edema formation. This speculation is based on the fact that it takes at least 24 hours until neutrophils infiltrate the injured brain and microglia gets activated and that it takes another 12-24 hours until monocytes and lymphocytes reach the injured brain in significant numbers and astrocytes start to release inflammatory cytokines and chemokines, [64-66] such as TNF, IL-6, IL-8 and IL-1β.

In summary, using *in vivo* 2-Photon microscopy in an established and highly standardized model of contusional TBI, we provided a detailed temporal and spatial characterization of the opening of the blood brain barrier after brain trauma. Increase of blood brain barrier permeability and subsequent vasogenic brain edema formation follow a biphasic pattern, suggesting an inevitable primary formation of vasogenic brain edema due to the initial injury of the brain and a secondary, more delayed formation of vasogenic brain edema due to so far unknown mechanism. Therefore, further studies using the currently developed imaging technology are needed to clarify which exact mechanisms are involved in post trauma BBB opening as a basis for the development of novel therapeutic strategies for patients suffering from vasogenic brain edema.

Acknowledgments

The authors would like to thank Uta Mamrak, Severin Filser and Igor Khalil for their valuable help in performing the experiments.

Disclosure

The authors report no competing financial interests.

References

1. Johnson, W.D. and Griswold, D.P. (2017). Traumatic brain injury: a global challenge. The Lancet Neurology 16, 949-950.

2. Thurman, D.J. (2016). The Epidemiology of Traumatic Brain Injury in Children and Youths: A Review of Research Since 1990. Journal of child neurology 31, 20-27.

3. Maas, A.I.R., Menon, D.K., Adelson, P.D., Andelic, N., Bell, M.J., Belli, A., Bragge, P., Brazinova, A., Buki, A., Chesnut, R.M., Citerio, G., Coburn, M., Cooper, D.J., Crowder, A.T., Czeiter, E., Czosnyka, M., Diaz-Arrastia, R., Dreier, J.P., Duhaime, A.C., Ercole, A., van Essen, T.A., Feigin, V.L., Gao, G., Giacino, J., Gonzalez-Lara, L.E., Gruen, R.L., Gupta, D., Hartings, J.A., Hill, S., Jiang, J.Y., Ketharanathan, N., Kompanje, E.J.O., Lanyon, L., Laureys, S., Lecky, F., Levin, H., Lingsma, H.F., Maegele, M., Majdan, M., Manley, G., Marsteller, J., Mascia, L., McFadyen, C., Mondello, S., Newcombe, V., Palotie, A., Parizel, P.M., Peul, W., Piercy, J., Polinder, S., Puybasset, L., Rasmussen, T.E., Rossaint, R., Smielewski, P., Soderberg, J., Stanworth, S.J., Stein, M.B., von Steinbuchel, N., Stewart, W., Steyerberg, E.W., Stocchetti, N., Synnot, A., Te Ao, B., Tenovuo, O., Theadom, A., Tibboel, D., Videtta, W., Wang, K.K.W., Williams, W.H., Wilson, L. and Yaffe, K. (2017). Traumatic brain injury: integrated approaches to improve prevention, clinical care, and research. Lancet Neurol 16, 987-1048.

4. Wilson, L., Stewart, W., Dams-O'Connor, K., Diaz-Arrastia, R., Horton, L., Menon, D.K. and Polinder, S. (2017). The chronic and evolving neurological consequences of traumatic brain injury. Lancet Neurol 16, 813-825.

5. Kaloostian, P., Robertson, C., Gopinath, S.P., Stippler, M., King, C.C., Qualls, C., Yonas, H. and Nemoto, E.M. (2012). Outcome prediction within twelve hours after severe traumatic brain injury by quantitative cerebral blood flow. Journal of neurotrauma 29, 727-734.

6. Sahuquillo, J., Poca, M.A. and Amoros, S. (2001). Current aspects of pathophysiology and cell dysfunction after severe head injury. Current pharmaceutical design 7, 1475-1503.

7. Maas, A.I., Stocchetti, N. and Bullock, R. (2008). Moderate and severe traumatic brain injury in adults. Lancet Neurol 7, 728-741.

8. Unterberg, A.W., Stover, J., Kress, B. and Kiening, K.L. (2004). Edema and brain trauma. Neuroscience 129, 1021-1029.

9. Jha, R.M. and Kochanek, P.M. (2018). A Precision Medicine Approach to Cerebral Edema and Intracranial Hypertension after Severe Traumatic Brain Injury: Quo Vadis? Current neurology and neuroscience reports 18, 105.

10. Jha, R.M., Kochanek, P.M. and Simard, J.M. (2019). Pathophysiology and treatment of cerebral edema in traumatic brain injury. Neuropharmacology 145, 230-246.
11. Stokum, J.A., Gerzanich, V. and Simard, J.M. (2016). Molecular pathophysiology of cerebral edema. J Cereb Blood Flow Metab 36, 513-538.
12. Marmarou, A. (2007). A review of progress in understanding the pathophysiology and treatment of brain edema. Neurosurgical focus 22, E1.
13. Winkler, E.A., Minter, D., Yue, J.K. and Manley, G.T. (2016). Cerebral Edema in Traumatic Brain Injury: Pathophysiology and Prospective Therapeutic Targets. Neurosurg Clin N Am 27, 473-488.
14. Lukaszewicz, A.C., Soyer, B. and Payen, D. (2011). Water, water, everywhere: sodium and water balance and the injured brain. Curr Opin Anaesthesiol 24, 138-143.
15. Hudak, A.M., Peng, L., Marquez de la Plata, C., Thottakara, J., Moore, C., Harper, C., McColl, R., Babcock, E. and Diaz-Arrastia, R. (2014). Cytotoxic and vasogenic cerebral oedema in traumatic brain injury: assessment with FLAIR and DWI imaging. Brain Inj 28, 1602-1609.
16. Alves, J.L. (2014). Blood-brain barrier and traumatic brain injury. J Neurosci Res 92, 141-147.
17. Katayama, Y. and Kawamata, T. (2003). Edema fluid accumulation within necrotic brain tissue as a cause of the mass effect of cerebral contusion in head trauma patients. Acta Neurochir Suppl 86, 323-327.
18. Blixt, J., Svensson, M., Gunnarson, E. and Wanecek, M. (2015). Aquaporins and blood-brain barrier permeability in early edema development after traumatic brain injury. Brain Res 1611, 18-28.
19. Ballabh, P., Braun, A. and Nedergaard, M. (2004). The blood-brain barrier: an overview: structure, regulation, and clinical implications. Neurobiol Dis 16, 1-13.
20. Donkin, J.J. and Vink, R. (2010). Mechanisms of cerebral edema in traumatic brain injury: therapeutic developments. Curr Opin Neurol 23, 293-299.
21. Schwarzmaier, S.M., Gallozzi, M. and Plesnila, N. (2015). Identification of the Vascular Source of Vasogenic Brain Edema following Traumatic Brain Injury Using In Vivo 2-Photon Microscopy in Mice. Journal of neurotrauma 32, 990-1000.
22. Terpolilli, N.A., Zweckberger, K., Trabold, R., Schilling, L., Schinzel, R., Tegtmeier, F. and Plesnila, N. (2009). The novel nitric oxide synthase inhibitor 4-amino-tetrahydro-L-biopterine

prevents brain edema formation and intracranial hypertension following traumatic brain injury in mice. Journal of neurotrauma 26, 1963-1975.
23. Schwarzmaier, S.M., Kim, S.W., Trabold, R. and Plesnila, N. (2010). Temporal profile of thrombogenesis in the cerebral microcirculation after traumatic brain injury in mice. Journal of neurotrauma 27, 121-130.
24. Guérin, C.J., Nolan, C.C., Mavroudis, G., Lister, T., Davidson, G.M., Holton, J.L. and Ray, D.E. (2001). The dynamics of blood–brain barrier breakdown in an experimental model of glial cell degeneration. Neuroscience 103, 873-883.
25. Reyes-Aldasoro, C.C., Wilson, I., Prise, V.E., Barber, P.R., Ameer-Beg, M., Vojnovic, B., Cunningham, V.J. and Tozer, G.M. (2008). Estimation of apparent tumor vascular permeability from multiphoton fluorescence microscopic images of P22 rat sarcomas in vivo. Microcirculation 15, 65-79.
26. Zweckberger, K., Eros, C., Zimmermann, R., Kim, S.W., Engel, D. and Plesnila, N. (2006). Effect of early and delayed decompressive craniectomy on secondary brain damage after controlled cortical impact in mice. Journal of neurotrauma 23, 1083-1093.
27. Shlosberg, D., Benifla, M., Kaufer, D. and Friedman, A. (2010). Blood-brain barrier breakdown as a therapeutic target in traumatic brain injury. Nature reviews. Neurology 6, 393-403.
28. Zweckberger, K., Stoffel, M., Baethmann, A. and Plesnila, N. (2003). Effect of decompression craniotomy on increase of contusion volume and functional outcome after controlled cortical impact in mice. Journal of neurotrauma 20, 1307-1314.
29. Murakami, K., Kondo, T., Yang, G., Chen, S.F., Morita-Fujimura, Y. and Chan, P.H. (1999). Cold injury in mice: a model to study mechanisms of brain edema and neuronal apoptosis. Progress in Neurobiology 57, 289-299.
30. Rosas-Hernandez, H., Cuevas, E., Escudero-Lourdes, C., Lantz, S.M., Gomez-Crisostomo, N.P., Sturdivant, N.M., Balachandran, K., Imam, S.Z., Slikker, W., Paule, M.G. and Ali, S.F. (2018). Characterization of Biaxial Stretch as an In Vitro Model of Traumatic Brain Injury to the Blood-Brain Barrier. Molecular Neurobiology 55, 258-266.
31. Yu, M., Wang, M., Yang, D., Wei, X. and Li, W. (2019). Dynamics of blood brain barrier permeability and tissue microstructure following controlled cortical impact injury in rat: A dynamic contrast-enhanced magnetic resonance imaging and diffusion kurtosis imaging study. Magn Reson Imaging 62, 1-9.

32. Shen, Q., Watts, L.T., Li, W. and Duong, T.Q. (2016). Magnetic Resonance Imaging in Experimental Traumatic Brain Injury. In: Injury Models of the Central Nervous System: Methods and Protocols. Kobeissy, F.H., Dixon, C.E., Hayes, R.L., Mondello, S. (eds). Springer New York: New York, NY, pps. 645-658.
33. Ren, Z., Shi, L., Wei, D. and Qiu, J. (2019). Brain Functional Basis of Subjective Well-being During Negative Facial Emotion Processing Task-Based fMRI. Neuroscience.
34. Wahl, M., Unterberg, A. and Baethmann, A. (1985). Intravital fluorescence microscopy for the study of blood-brain-barrier function. Int J Microcirc Clin Exp 4, 3-18.
35. Mayhan, W.G. and Heistad, D.D. (1985). Permeability of blood-brain barrier to various sized molecules. Am J Physiol 248, H712-718.
36. Prager, O., Chassidim, Y., Klein, C., Levi, H., Shelef, I. and Friedman, A. (2010). Dynamic in vivo imaging of cerebral blood flow and blood-brain barrier permeability. Neuroimage 49, 337-344.
37. Klohs, J., Steinbrink, J., Bourayou, R., Mueller, S., Cordell, R., Licha, K., Schirner, M., Dirnagl, U., Lindauer, U. and Wunder, A. (2009). Near-infrared fluorescence imaging with fluorescently labeled albumin: a novel method for non-invasive optical imaging of blood-brain barrier impairment after focal cerebral ischemia in mice. J Neurosci Methods 180, 126-132.
38. Saunders, N.R., Dziegielewska, K.M., Møllgård, K. and Habgood, M.D. (2015). Markers for blood-brain barrier integrity: how appropriate is Evans blue in the twenty-first century and what are the alternatives? Frontiers in neuroscience 9, 385.
39. Schwarzmaier, S.M., Zimmermann, R., McGarry, N.B., Trabold, R., Kim, S.-W. and Plesnila, N. (2013). In vivo temporal and spatial profile of leukocyte adhesion and migration after experimental traumatic brain injury in mice. Journal of Neuroinflammation 10, 1-17.
40. Schwarzmaier, S.M., Terpolilli, N.A., Dienel, A., Gallozzi, M., Schinzel, R., Tegtmeier, F. and Plesnila, N. (2015). Endothelial nitric oxide synthase mediates arteriolar vasodilatation after traumatic brain injury in mice. Journal of neurotrauma 32, 731-738.
41. Schwarzmaier, S.M. and Plesnila, N. (2014). Contributions of the immune system to the pathophysiology of traumatic brain injury - evidence by intravital microscopy. Front Cell Neurosci 8, 358.
42. Allt, G. and Lawrenson, J.G. (1997). Is the pial microvessel a good model for blood-brain barrier studies? Brain research. Brain research reviews 24, 67-76.

43. Helmchen, F. (2009). Frontiers in Neuroscience,Two-Photon Functional Imaging of Neuronal Activity. In: In Vivo Optical Imaging of Brain Function. nd, Frostig, R.D. (eds). CRC Press/Taylor & Francis, Taylor & Francis Group, LLC.: Boca Raton (FL).
44. Barzo, P., Marmarou, A., Fatouros, P., Corwin, F. and Dunbar, J. (1996). Magnetic resonance imaging-monitored acute blood-brain barrier changes in experimental traumatic brain injury. J Neurosurg 85, 1113-1121.
45. Shapira, Y., Setton, D., Artru, A.A. and Shohami, E. (1993). Blood-brain barrier permeability, cerebral edema, and neurologic function after closed head injury in rats. Anesth Analg 77, 141-148.
46. Baskaya, M.K., Rao, A.M., Dogan, A., Donaldson, D. and Dempsey, R.J. (1997). The biphasic opening of the blood-brain barrier in the cortex and hippocampus after traumatic brain injury in rats. Neurosci Lett 226, 33-36.
47. Habgood, M.D., Bye, N., Dziegielewska, K.M., Ek, C.J., Lane, M.A., Potter, A., Morganti-Kossmann, C. and Saunders, N.R. (2007). Changes in blood-brain barrier permeability to large and small molecules following traumatic brain injury in mice. The European journal of neuroscience 25, 231-238.
48. Baldwin, S.A., Fugaccia, I., Brown, D.R., Brown, L.V. and Scheff, S.W. (1996). Blood-brain barrier breach following cortical contusion in the rat. Journal of neurosurgery 85, 476-481.
49. Yeoh, S., Bell, E.D. and Monson, K.L. (2013). Distribution of blood-brain barrier disruption in primary blast injury. Annals of biomedical engineering 41, 2206-2214.
50. Tanno, H., Nockels, R.P., Pitts, L.H. and Noble, L.J. (1992). Breakdown of the blood-brain barrier after fluid percussive brain injury in the rat. Part 1: Distribution and time course of protein extravasation. Journal of neurotrauma 9, 21-32.
51. Korn, A., Golan, H., Melamed, I., Pascual-Marqui, R. and Friedman, A. (2005). Focal cortical dysfunction and blood-brain barrier disruption in patients with Postconcussion syndrome. Journal of clinical neurophysiology : official publication of the American Electroencephalographic Society 22, 1-9.
52. Strbian, D., Durukan, A., Pitkonen, M., Marinkovic, I., Tatlisumak, E., Pedrono, E., Abo-Ramadan, U. and Tatlisumak, T. (2008). The blood-brain barrier is continuously open for several weeks following transient focal cerebral ischemia. Neuroscience 153, 175-181.

53. Tomkins, O., Shelef, I., Kaizerman, I., Eliushin, A., Afawi, Z., Misk, A., Gidon, M., Cohen, A., Zumsteg, D. and Friedman, A. (2008). Blood-brain barrier disruption in post-traumatic epilepsy. J Neurol Neurosurg Psychiatry 79, 774-777.
54. Zlotnik, A., Klin, Y., Gruenbaum, B.F., Gruenbaum, S.E., Ohayon, S., Leibowitz, A., Kotz, R., Dubilet, M., Boyko, M., Shapira, Y. and Teichberg, V.I. (2012). b2 Adrenergic-mediated Reduction of Blood Glutamate Levels and Improved Neurological Outcome After Traumatic Brain Injury in Rats. J Neurosurg Anesthesiol 24, 30–38.
55. Gerzanich, V., Stokum, J.A., Ivanova, S., Woo, S.K., Tsymbalyuk, O., Sharma, A., Akkentli, F., Imran, Z., Aarabi, B., Sahuquillo, J. and Simard, J.M. (2019). Sulfonylurea Receptor 1, Transient Receptor Potential Cation Channel Subfamily M Member 4, and KIR6.2:Role in Hemorrhagic Progression of Contusion. Journal of neurotrauma 36, 1060-1079.
56. Rodriguez-Baeza, A., Reina-de la Torre, F., Poca, A., Marti, M. and Garnacho, A. (2003). Morphological features in human cortical brain microvessels after head injury: a three-dimensional and immunocytochemical study. Anat Rec A Discov Mol Cell Evol Biol 273, 583-593.
57. Sangiorgi, S., De Benedictis, A., Protasoni, M., Manelli, A., Reguzzoni, M., Cividini, A., Dell'orbo, C., Tomei, G. and Balbi, S. (2013). Early-stage microvascular alterations of a new model of controlled cortical traumatic brain injury: 3D morphological analysis using scanning electron microscopy and corrosion casting. Journal of neurosurgery 118, 763-774.
58. Adelson, P.D., Whalen, M.J., Kochanek, P.M., Robichaud, P. and Carlos, T.M. (1998). Blood brain barrier permeability and acute inflammation in two models of traumatic brain injury in the immature rat: a preliminary report. Acta Neurochir Suppl 71, 104-106.
59. Soares, H.D., Hicks, R.R., Smith, D. and McIntosh, T.K. (1995). Inflammatory leukocytic recruitment and diffuse neuronal degeneration are separate pathological processes resulting from traumatic brain injury. The Journal of neuroscience : the official journal of the Society for Neuroscience 15, 8223-8233.
60. Roth, T.L., Nayak, D., Atanasijevic, T., Koretsky, A.P., Latour, L.L. and McGavern, D.B. (2014). Transcranial amelioration of inflammation and cell death after brain injury. Nature 505, 223-228.
61. McDonald, B., Pittman, K., Menezes, G.B., Hirota, S.A., Slaba, I., Waterhouse, C.C., Beck, P.L., Muruve, D.A. and Kubes, P. (2010). Intravascular danger signals guide neutrophils to sites of sterile inflammation. Science 330, 362-366.

62. Semple, B.D., Bye, N., Rancan, M., Ziebell, J.M. and Morganti-Kossmann, M.C. (2010). Role of CCL2 (MCP-1) in traumatic brain injury (TBI): evidence from severe TBI patients and CCL2-/- mice. Journal of cerebral blood flow and metabolism : official journal of the International Society of Cerebral Blood Flow and Metabolism 30, 769-782.
63. da Fonseca, A.C., Matias, D., Garcia, C., Amaral, R., Geraldo, L.H., Freitas, C. and Lima, F.R. (2014). The impact of microglial activation on blood-brain barrier in brain diseases. Frontiers in cellular neuroscience 8, 362.
64. Corrigan, F., Mander, K.A., Leonard, A.V. and Vink, R. (2016). Neurogenic inflammation after traumatic brain injury and its potentiation of classical inflammation. J Neuroinflammation 13, 264.
65. Jassam, Y.N., Izzy, S., Whalen, M., McGavern, D.B. and El Khoury, J. (2017). Neuroimmunology of Traumatic Brain Injury: Time for a Paradigm Shift. Neuron 95, 1246-1265.
66. Simon, D.W., McGeachy, M.J., Bayir, H., Clark, R.S., Loane, D.J. and Kochanek, P.M. (2017). The far-reaching scope of neuroinflammation after traumatic brain injury. Nature reviews. Neurology 13, 171-191.

Figure 1

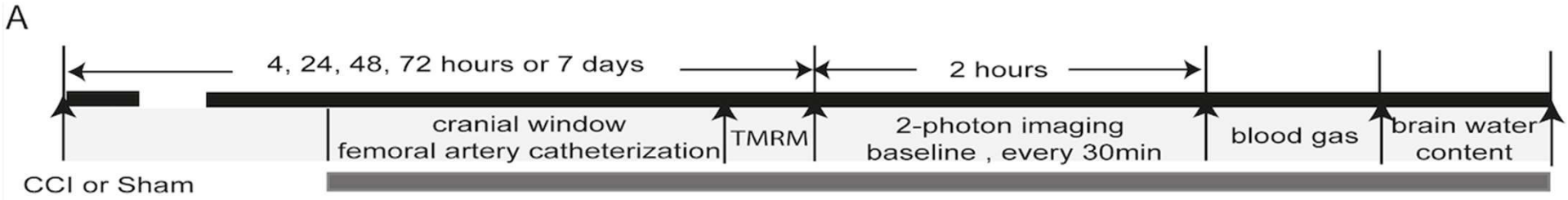
A
4, 24, 48, 72 hours or 7 days
2 hours
cranial window
femoral artery catheterization
TMRM
2-photon imaging
baseline , every 30min
blood gas
brain water
content
CCI or Sham

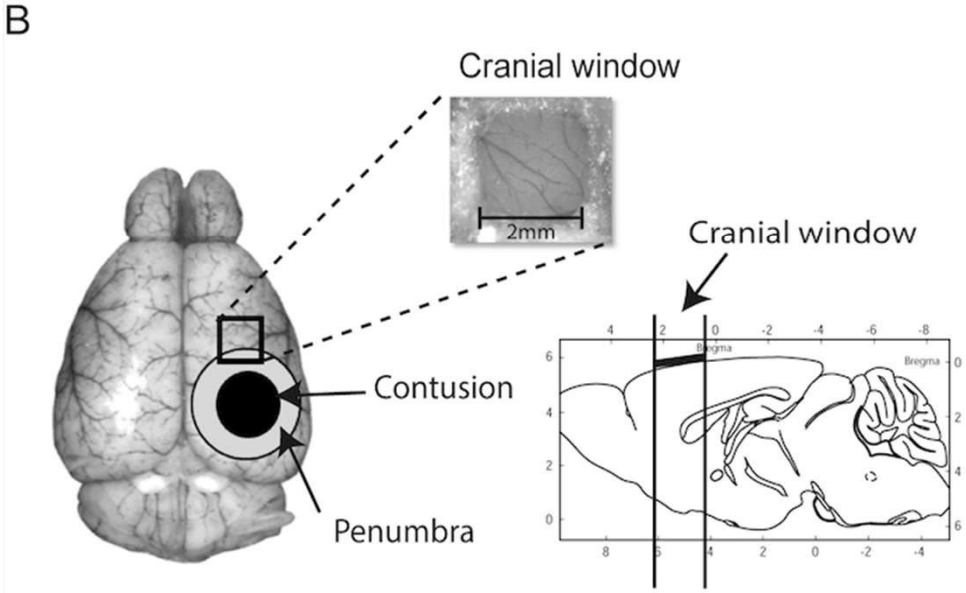
B
Cranial window
2mm
Cranial window
Contusion
Penumbra
Bregma
Bregma

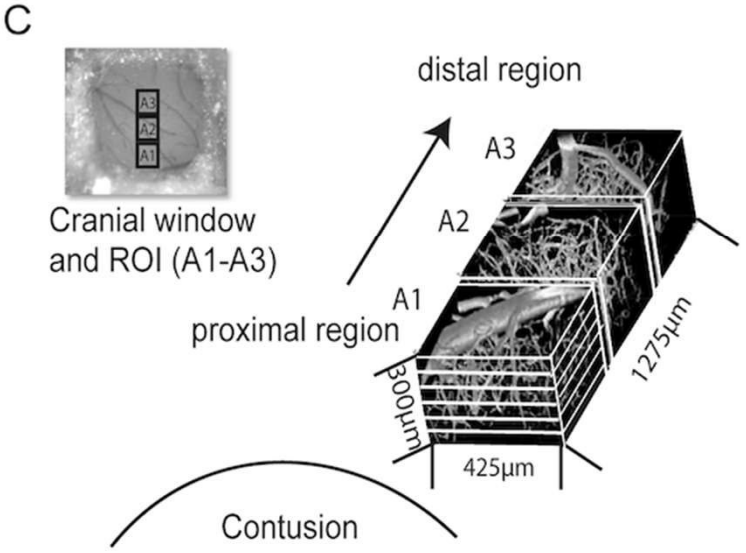
C
A3
A2
A1
Cranial window
and ROI (A1-A3)
distal region
A3
A2
A1
proximal region
300µm
1275µm
425µm
Contusion

Figure 2

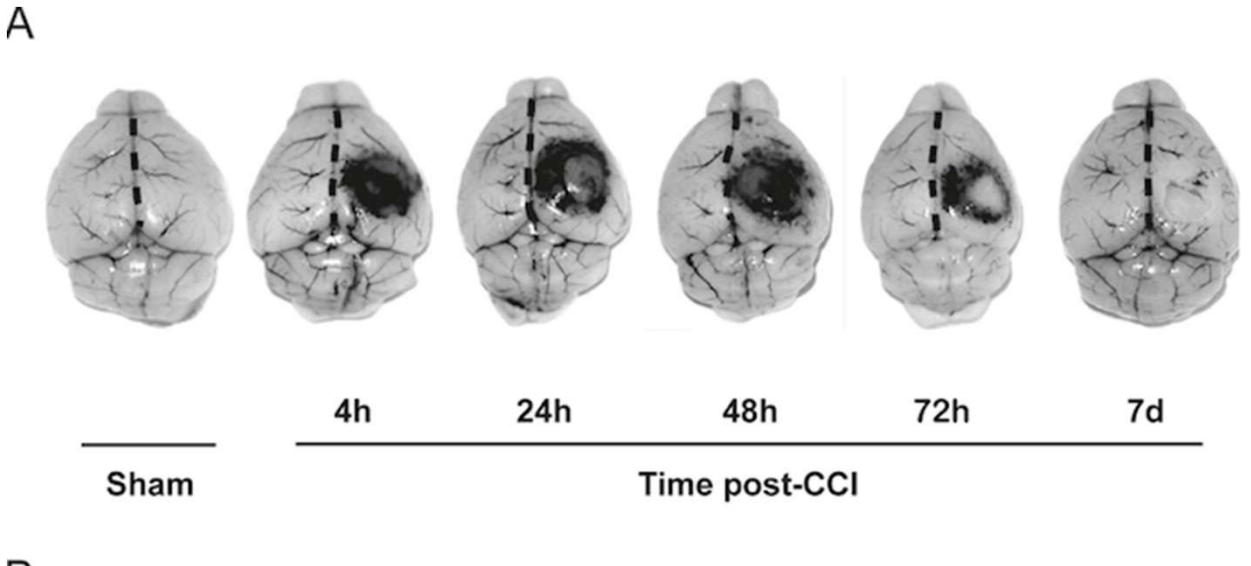
A
4h
24h
48h
72h
7d
Sham
Time post-CCI
B
contralateral
Ipsilateral
n=5-6; mean+/-SD
* P<0.05 vs sham
Brain water content (%)
86
84
82
80
78
76
74
sham
4h
24h
48h
72h
7d
Time post-CCI

Figure 3

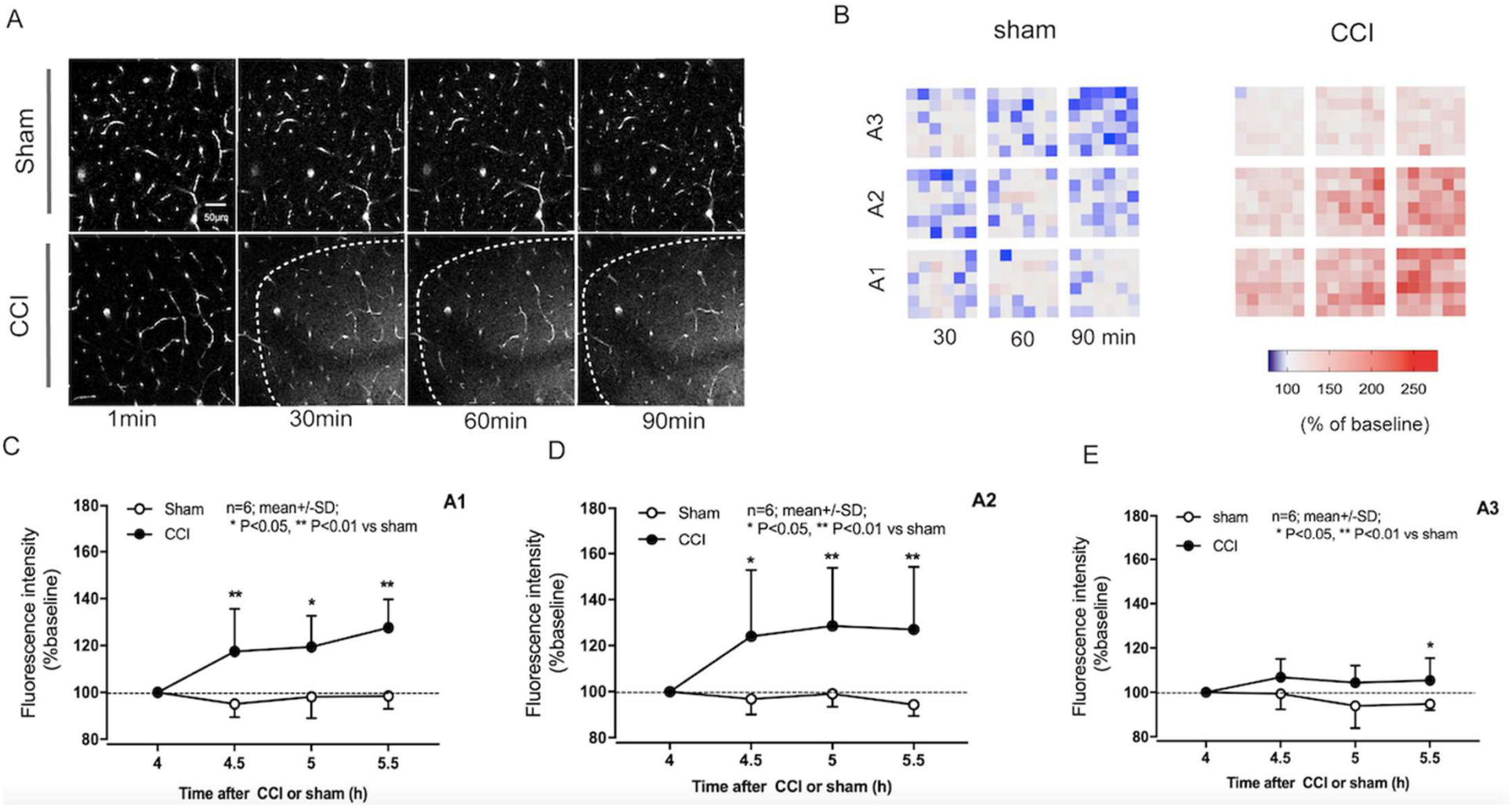
A
Sham
CCI
50μm
1min
30min
60min
90min
B
sham
CCI
A3
A2
A1
30
60
90 min
100 150 200 250
(% of baseline)
C
A1
Sham
CCI
n=6; mean+/-SD;
* P<0.05, ** P<0.01 vs sham
Fluorescence intensity (%baseline)
Time after CCI or sham (h)
D
A2
Sham
CCI
n=6; mean+/-SD;
* P<0.05, ** P<0.01 vs sham
Fluorescence intensity (%baseline)
Time after CCI or sham (h)
E
A3
sham
CCI
n=6; mean+/-SD;
* P<0.05, ** P<0.01 vs sham
Fluorescence intensity (%baseline)
Time after CCI or sham (h)

Figure 4

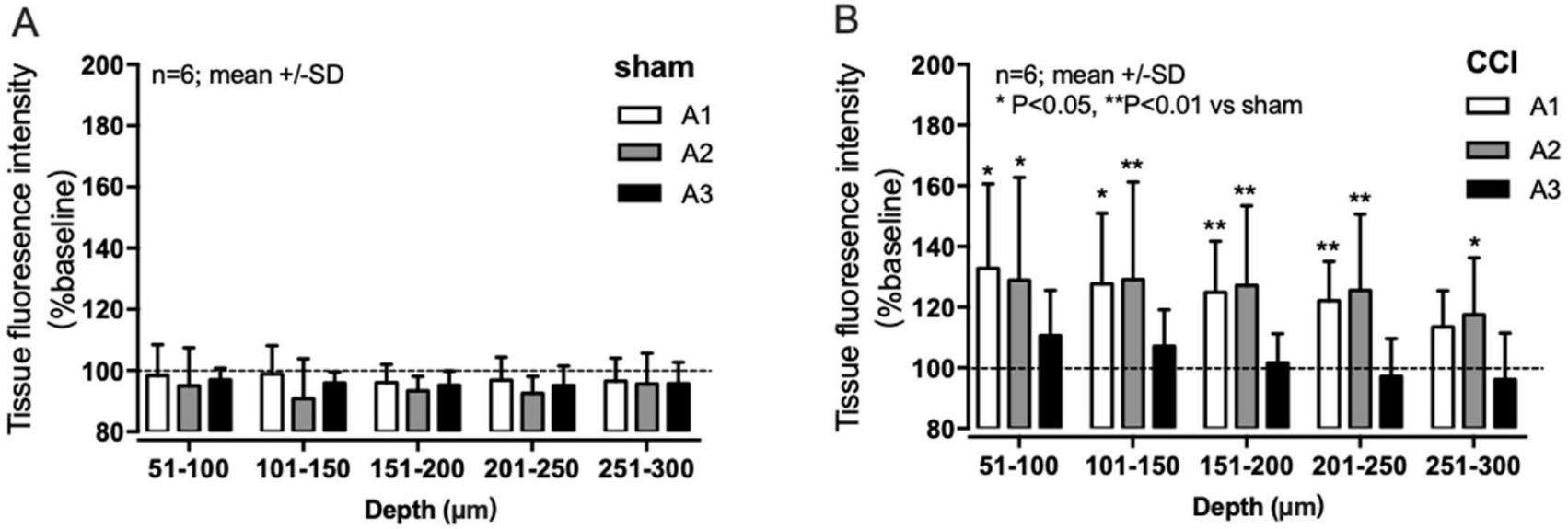
A
n=6; mean +/-SD
sham
A1
A2
A3
Tissue fluoresence intensity (%baseline)
200
180
160
140
120
100
80
51-100
101-150
151-200
201-250
251-300
Depth (µm)
B
n=6; mean +/-SD
* P<0.05, **P<0.01 vs sham
CCI
A1
A2
A3
Tissue fluoresence intensity (%baseline)
Depth (µm)

Figure 5

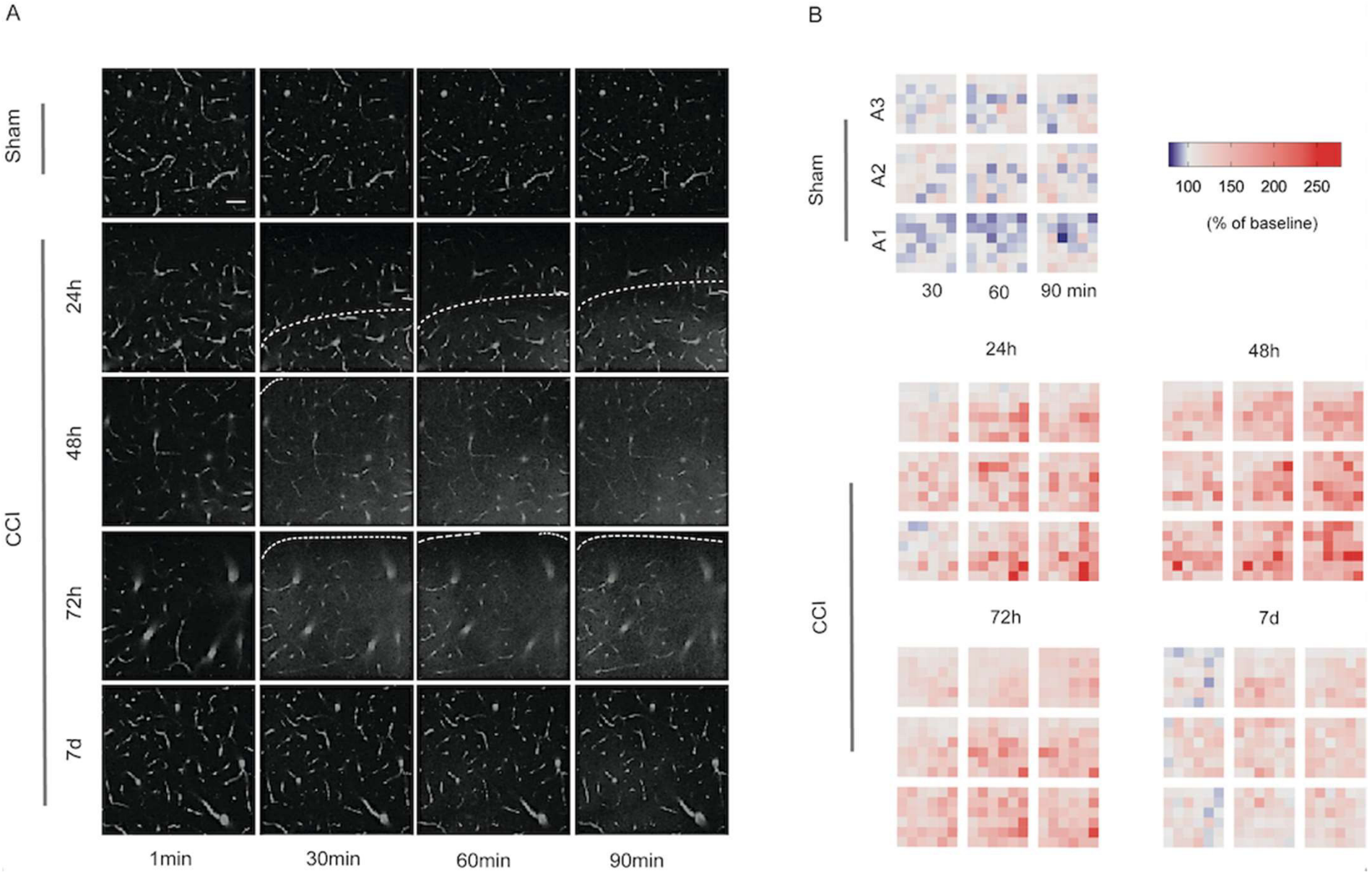
A
Sham
CCI
24h
48h
72h
7d
1min
30min
60min
90min
B
Sham
A3
A2
A1
30
60
90 min
100
150
200
250
(% of baseline)
CCI
24h
48h
72h
7d

Figure 6

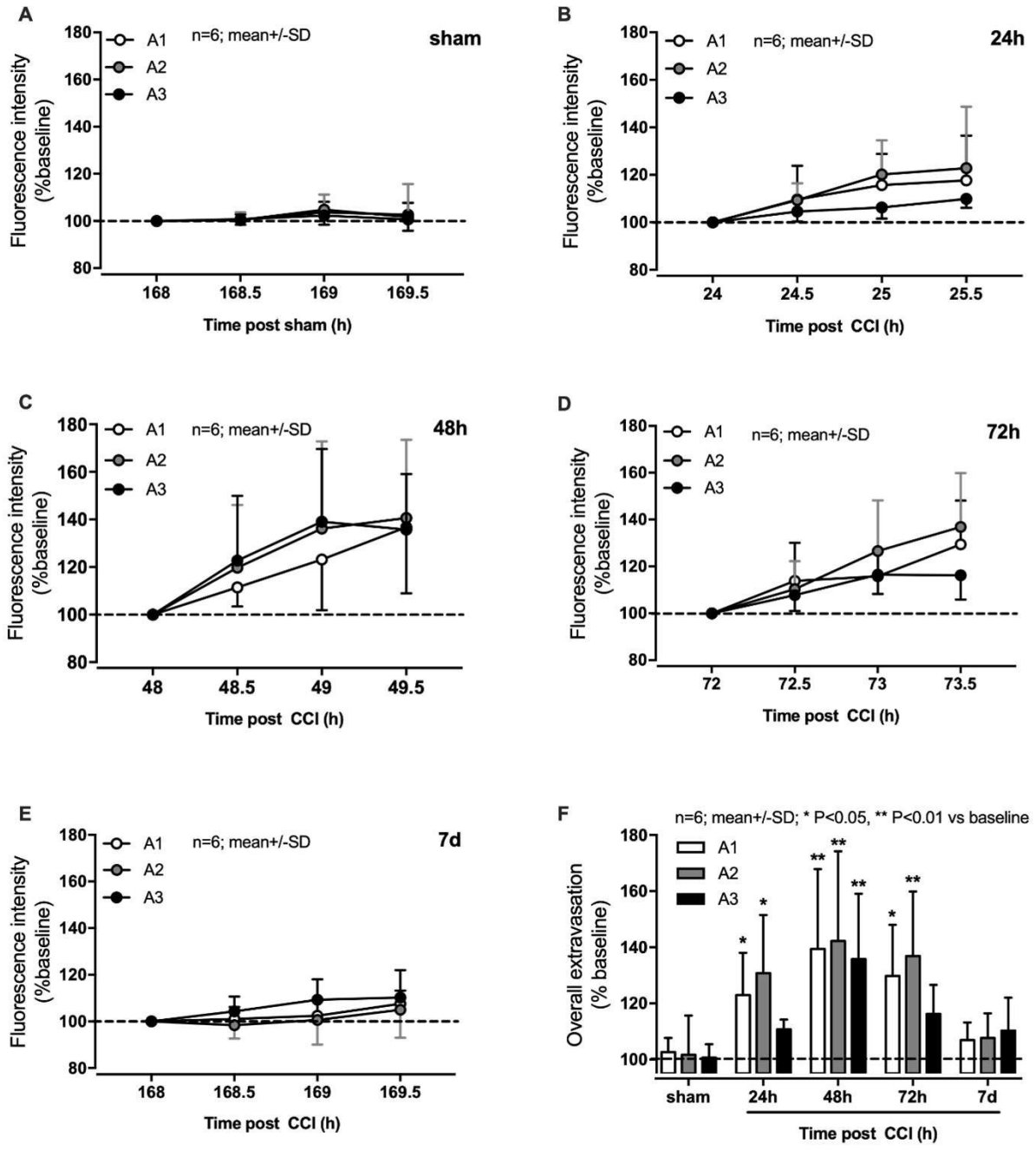
A
B
C
D
E
F
A1
A2
A3
n=6; mean+/-SD
sham
24h
48h
72h
7d
Fluorescence intensity (%baseline)
Time post sham (h)
Time post CCI (h)
n=6; mean+/-SD; * P<0.05, ** P<0.01 vs baseline
Overall extravasation (% baseline)
sham
24h
48h
72h
7d

Figure 7

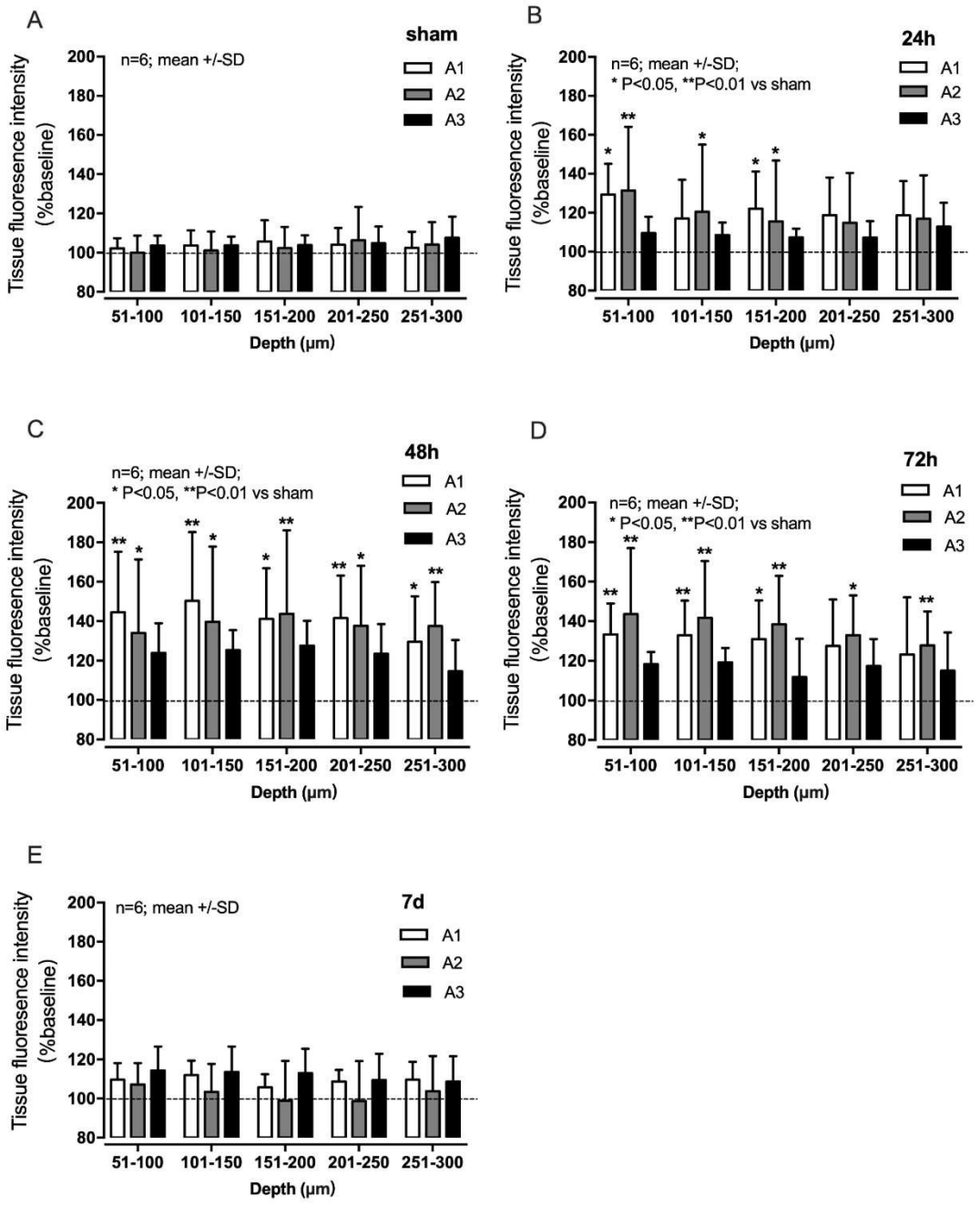
A
sham
n=6; mean +/-SD
A1
A2
A3
Tissue fluoresence intensity (%baseline)
200
180
160
140
120
100
80
51-100
101-150
151-200
201-250
251-300
Depth (µm)
B
24h
n=6; mean +/-SD;
* P<0.05, **P<0.01 vs sham
C
48h
D
72h
E
7d

Figure 8

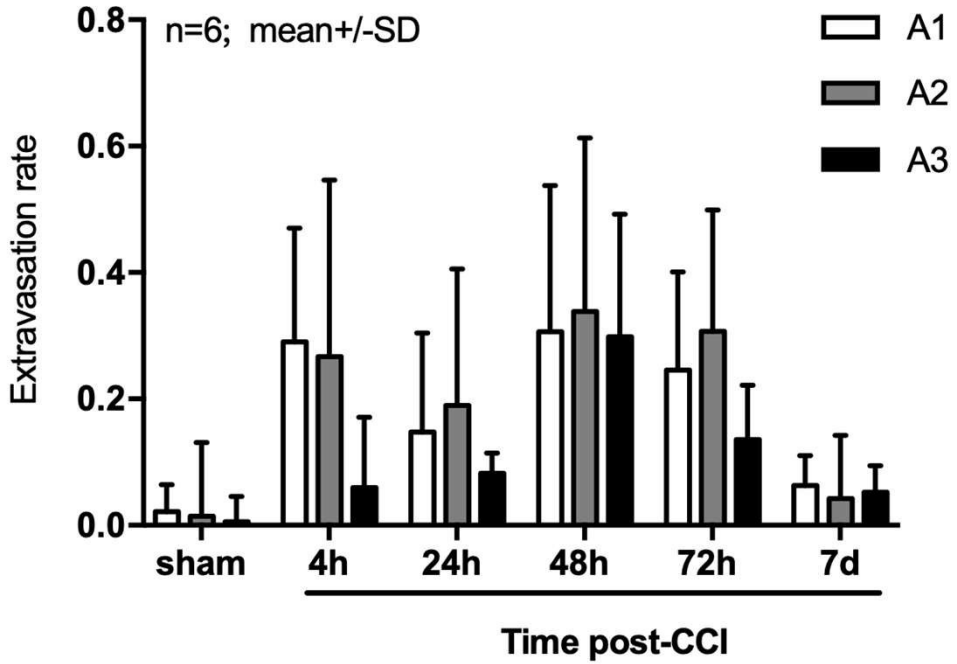
n=6; mean+/-SD
A1
A2
A3
Extravasation rate
0.8
0.6
0.4
0.2
0.0
sham
4h
24h
48h
72h
7d
Time post-CCI

Supplementary 1

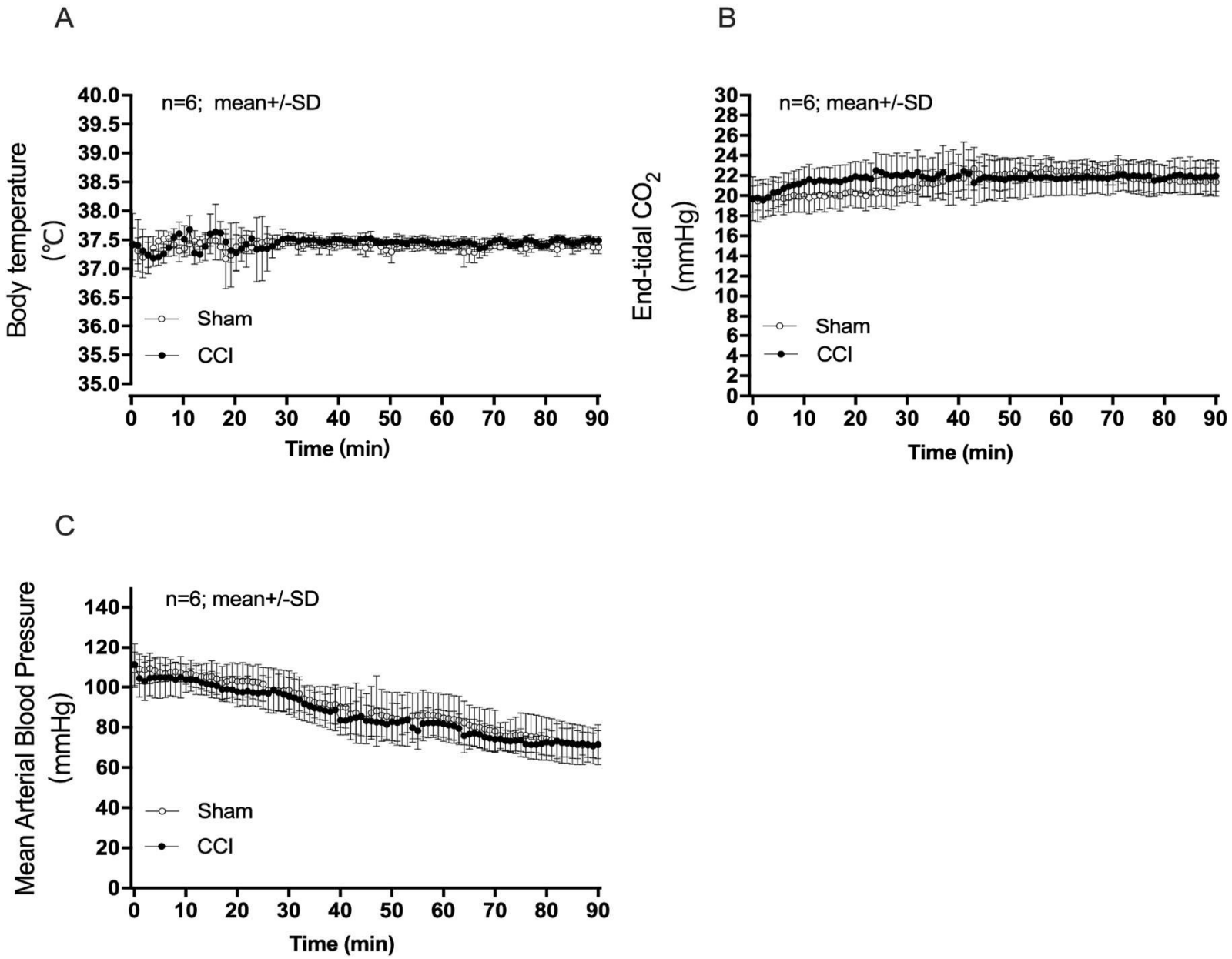

Supplementary 2

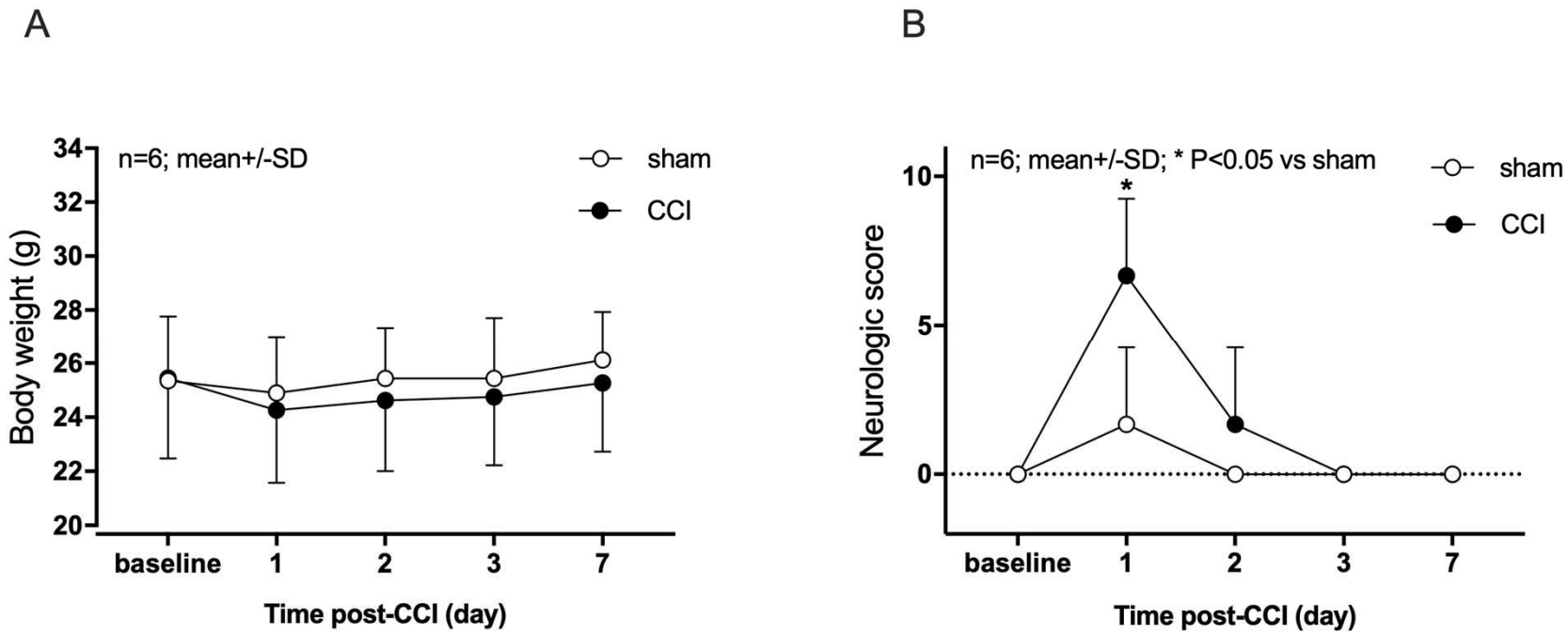

Supplementary 3

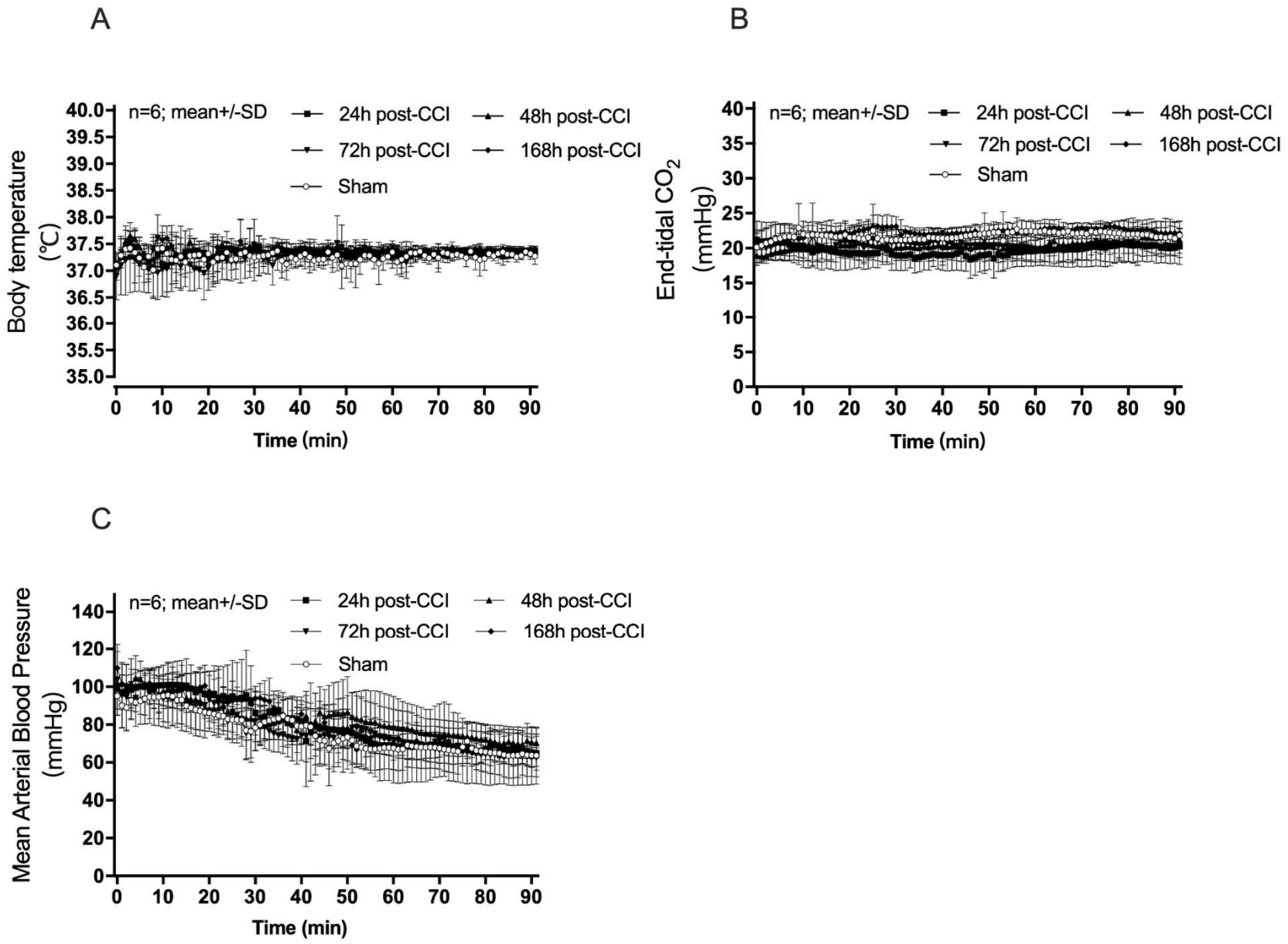

Figure legends

Figure 1 Experimental setup. (A) Timeline of the experimental series investigating the short– and long-term development of vasogenic brain edema formation. Body weight and neurologic score were assessed at day 1, day 2, day 3 and day 7 following CCI. (B) Location of the contusion (black), the penumbra (gray), and the cranial window on the brain. (C) Scheme of the location of the ROI for imaging (A1-A3) with A1 being the most proximal region to the contusion. For each area, the side length was 425 µm x 425 µm and all areas extended vertically from the surface to a depth of 300µm into the parenchyma. 6 layers were separated by depth (0 µm-300 µm).

Figure 2 Brain swelling following CCI at different time points. (A) Gross anatomy pictures showing the contusion and midline shift at different time points following CCI. Hematoma formation is visible on the surface. (B) Water content in the injured hemisphere and control hemisphere at different time points after TBI. SD= standard deviation; ns $P>0.05$, *$P<0.05$ (vs sham ipsilateral).

Figure 3 Short-term development of vasogenic brain edema formation after CCI or sham operation (4h). A) Representative images from area A1, at a depth of 150 µm; scale bar: 50µm Vessels were labeled with TMRM. No extravasation is visible after sham operation. In contrast, the extravasation of TMRM is clearly visible 4.5h following CCI. B) Color map indicating the fluorescence intensity in % baseline in the gridded (6x6) ROI according to the maximum intensity projection. C) Extravasation of TMRM in different areas (A1-A3) over time (4h). Fluorescent signal intensity increased over time in A1 and A2 (A-B), compared to sham operation. However, in the most distal region A3 TMRM extravasation was less strong. The dotted line represents the baseline. SD=standard deviation. *$P<0.05$, **$P<0.01$ (vs sham).

Figure 4 Extravasation of TMRM in the depth at 5.5h following trauma or sham operation (i.e. the last measuring point in the short-term groups). Fluorescence intensity was assessed in 5 layers reaching from 50 µm to 300 µm into the brain (excluding the most superficial layer). The dotted line represents the baseline. SD=standard deviation. *P<0.05, **P<0.01 (vs sham).

Figure 5 Long-term development of vasogenic brain edema formation after CCI or sham operation (24h-7d). A) Representative images from area A1, at a depth of 150 µm; scale bar: 50µm. Vessels were labeled with TMRM. B) Color map indicating the fluorescence intensity in % baseline in the gridded (6x6) ROI according to the maximum intensity projection.

Figure 6 Extravasation of TMRM in different areas (A1-A3) over time (24h-7d). TMRM extravasation is depicted as fluorescence increase in percent of the baseline fluorescence. Quantification of extravasation at different time points following sham-operated mice (A) or CCI (B-E). (F) Overall fluorescence intensity in the different groups. SD=standard deviation. *P<0.05, **P<0.01 (vs sham).

Figure 7 Extravasation of TMRM in the depth at different time points following CCI or sham operation (24h-7d). Fluorescent intensity was assessed in 5 layers reaching from 50 µm to 300 µm into the brain (excluding the most superficial layer reaching 0–50 µm). SD=standard deviation. *P<0.05, **P<0.01 (vs sham).

Figure 8 Average rate of extravasation after CCI or sham operation at different time points following CCI. SD=standard deviation. Extravasation rate is presented as *change of fluorescence intensity per minute.* BBB permeability increase after TBI follows a biphasic pattern.

Supplementary 1 Physiological parameters during imaging (short-term series). Core body temperature (A), end-tidal CO_2 (B), and mean arterial blood pressure (C) were monitored continuously throughout the experiment and kept within the physiological range.

Supplementary 2 Body weight (A) and General condition/neurologic score (B) were determined at day 1, day 2, day 3 and day 7 following CCI or sham operation in the 7 day groups.

Supplementary 3 Physiological parameters during imaging (Longer-term 24h-7d). Core body temperature (A), end-tidal CO_2 (B), and mean arterial blood pressure (C) were monitored continuously throughout the experiment and kept within the physiological range.